Research Article

Rapid Communications in Mass Spectrometry

Received: 16 November 2010 Revised: 4 January 2011 Accepted: 5 January 2011 Published online in Wiley Online Library: 00 Month 2011

Rapid Commun. Mass Spectrom. **2011**, *25*, 877–888
(wileyonlinelibrary.com) DOI: 10.1002/rcm.4931

A new liquid chromatography/electrospray ionization mass spectrometry method for the analysis of underivatized aliphatic long-chain polyamines: application to diatom-rich sediments

Maxime C. Bridoux[1], Vadim V. Annenkov[2], Henning Menzel[3], Richard G. Keil[1] and Anitra E. Ingalls[1]*

[1]School of Oceanography, Box 355351, University of Washington, Seattle, WA 98195, USA
[2]Limnological Institute of the Siberian Branch of the Russian Academy of Sciences, 3 Ulan-Batorskaya St., P.O. Box 278, Irkusk 664033, Russia
[3]Institute of Technical Chemistry, Technical University of Braunschweig, Hans-Sommer-Str. 10, 38106 Braunschweig, Germany

Natural polyamines are found in all three domains of life and long-chain polyamines (LCPAs) play a special role in silicifying organisms such as diatoms and sponges where they are actively involved in the complex formation and nanopatterning of siliceous structures. With chain lengths extending up to 20 N-methylated propylamine repeat units, diatom LCPAs constitute the longest natural polyamines. Mixtures of natural LCPAs are typically purified in bulk using ion-exchange, size-exclusion and dialysis and then analyzed either by direct infusion mass spectrometry or by MALDI-TOF. Here, we describe a novel ion-pairing liquid chromatographic method that allows baseline separation, detection and structural elucidation of underivatized aliphatic methylated and non-methylated LCPAs with a wide range of chain lengths. Complete separation of synthetic mixtures of LCPA species differing by either a propylamine or an *N*-methylpropylamine unit is achievable using this method and chromatographic separation of natural, diatom frustule bound LCPAs extracted from sediment core samples is greatly improved. Using electrospray ionization mass spectrometry (ESI-MS), we detected singly $[M+H]^+$ and multiply $[M+nH]^{n+}$ charged protonated ions. The abundance of multiply charged LCPA species increased linearly as a function of LCPA chain length (N) and multiprotonated ions $[M+nH]^{n+}$ were more abundant for longer chain polyamines. The abundance of multiply charged LCPAs along with the concomitant disappearance of the singly charged protonated molecular ion significantly increases the complexity of the MS spectra, justifying the need for good chromatographic separation of complex LCPA mixtures. This analytical procedure will likely constitute a powerful tool for the characterization, quantification, as well as the purification of individual LCPAs in natural and synthetic samples for studies of silica precipitation as well as nitrogen and carbon isotopic analysis used in paleoceanographic studies.

Naturally occurring polyamines constitute a ubiquitous class of natural bioactive polycationic compounds with primary and secondary amines, synthesized by all living cells. The most common aliphatic polyamines in eukaryotic cells are the short-chain putrescine, spermidine and spermine. Prokaryotes (Archaea and Bacteria) synthesize a tetraamine isomer of spermine called thermospermine, whose presence has also been detected in lower eukaryotes and plants.[1–5] While those common short-chain polyamines have extensively been studied due to their essential functions in cellular processes, aliphatic long-chain polyamines (LCPAs) are less common but also appear in each domain of life.[2,3,5] LCPAs were isolated for the first time from the frustules of the marine diatom *Cylindrotheca fusiformis* only a decade ago.[6] Since then, research focusing on LCPAs has increased and clearly established their widespread occurrence in silicifying organisms and their role in the formation of hierarchically structured silica-based diatom frustules[4,7–9] and sponge spicules.[10]

In diatoms, LCPAs are assumed to be part of a self-assembled nanostructured organic matrix located within the silica deposition vesicle (SDV) lumen.[11] LCPAs can be covalently bound to the lysine residues of silaffins[6] (proteins responsible for biomineralization of diatom frustules) but most LCPAs are found in the free form, associated with biosilica. This organic matrix accelerates silica formation and acts as a template for the formation of three-dimensional silica structures.[11] In sponges, LCPAs also appear to be covalently bound to other, unidentified high molecular weight compounds.[10] During precipitation, LCPAs are incorporated in biosilica, allowing them to persist in the environment for long time periods.[12,13]

The biochemical pathways leading to the biosynthesis of LCPAs are still unclear. However, a recent study showed that

* *Correspondence to*: A. E. Ingalls, School of Oceanography, Box 355351, University of Washington, Seattle, WA 98195, USA. E-mail: aingalls@u.washington.edu

a specific inhibitor of the enzyme *ornithine decarboxylase* resulted in the alteration of the silica structure in the frustule of the marine diatom *T. pseudonana*, suggesting that LCPAs likely derive from the spermidine/spermine pathway.[14] To date, the polyamine composition of seven marine diatom species (including the following genera: *Chaetoceros*, *Coscinodiscus*, *Cylindrotheca*, *Eucampia*, *Navicula*, *Stephanopyxis* and *Thalassiosira*) and two marine sponge species (*Axinyssa aculeate* and *Halichondra* spp.) revealed a consistent pattern of N-methylated derivatives of oligo-propyleneimine chains attached to a putrescine, ornithine, propylamine, spermine, spermidine and 1,3-diaminopropane.[10,11] Each diatom species was found to contain LCPAs that exhibit characteristic chain lengths, variations in the degree of N-methylation, position of secondary and tertiary amino functionalities, as well as incorporation of site-specific quaternary ammonium groups.[8,15] The methylation pattern of LCPAs affects the kinetics of silicic acid condensation[16] and LCPA chain length and N-to-N spacing distance influence the amount of silica precipitated.[17]

LCPAs in biosilica are typically released by HF or NH_4F dissolution of the biosilica, purified using ion-exchange, size-exclusion chromatography, dialysis and polyacrylamide gel electrophoresis (SDS-PAGE). The bands are then excised, reconstituted with the appropriate solvent and either infused directly in the ion source of the mass spectrometer or analyzed by matrix-assisted laser desorption/ionization (MALDI).[4,6,8,10,15]

Analysis of polyamines by reversed-phase high-performance liquid chromatography (HPLC)-based methods is challenging due to the high polarity of those compounds. Also, polyamine detection typically requires pre- or post-column derivatization, when using UV or fluorescence detection, since the polyamine backbone does not display native fluorescence and it absorbs UV light at the same wavelength where interfering compounds are detectable.[18] Besides, derivatization of long-chain polyamines is not a practical approach due to the high number of primary and secondary amines.

Liquid chromatography coupled to mass spectrometry (LC/MS) allows identification of underivatized LCPAs based on retention time, molecular weight and characteristic ion fragmentation patterns. We recently presented an LC/MS-based method that uses the ion-pairing reagent heptafluorobutyric acid and a reversed-phase C_{18} column for the underivatized analysis of LCPAs extracted from Southern Ocean sediment cores.[13] However, chromatographic separation of individual LCPA components was not achieved and all LCPAs eluted in one broad chromatographic peak.

Here, we report an improved HPLC method for the complete separation of underivatized LCPAs. We used two different synthetic polypropyleneimine standard mixtures to achieve good separation of individual methylated and non-methylated LCPAs and then applied that separation scheme to a diatom frustule-rich marine sediment sample from core TNO57-13 collected in the Atlantic sector of the Southern Ocean. Mass spectrometric analysis of LCPAs using tandem mass spectrometry (MS/MS) revealed previously unidentified multiply charged LCPA species.

EXPERIMENTAL

LCPA standards

Long-chain polyamines containing *N*-methylpropylamines (standard mixture B) were synthesized via condensation reactions using N1,N3-dimethyl-N1-[3-(methylamino)propyl]-1,3-propanediamine and 1,3-dibromopropane.[19]

Synthetic polyamines containing polypropyleneimine (standard mixture A) were synthesized by ring-opening polymerization of 1,3-oxazine monomers followed by sodium hydroxide hydrolysis.[20]

LCPAs extracted from a Southern Ocean sediment core

Fossil LCPAs were extracted from the 799–801 cm depth interval of a diatom frustule-rich sediment core, TNO57-13PC4 (corresponding to approximately 17 000 years). TNO57-13PC4 was recovered from the Atlantic sector of the Southern Ocean (53.2°S 5.1°E). The sediments were chemically cleaned of exogenous organic material.[13] In brief, sediments were sequentially extracted three times each in 6 mL MeOH, then 6 mL DCM/MeOH and finally in 6 mL DCM, in Teflon centrifuge tubes. Samples were vortexed, sonicated (5 min in an ultrasonic bath) and centrifuged at 12 000 *g* for 5 min between each solvent extraction step to form a pellet. The pellet was then rinsed with milli-Q water and acid hydrolyzed in 6 N HCl for 20 h at 110°C. The cleaned frustules were rinsed with milli-Q water until neutral pH was obtained and were freeze-dried. Concentrated HF (3 mL/g opal) was added to 1.5 g freeze-dried opal, to completely dissolve the sample and release organic compounds incorporated within the hydrated silica matrix. The resulting solution was then concentrated to dryness using a CentriVap. The dried residue containing LCPAs was dissolved in 1 mL milli-Q water, filtered through a 0.2-μm Teflon syringe filter and subjected to liquid chromatography/mass spectrometry (LC/MS).

LC/MS instruments and conditions

Aliphatic long-chain polyamine synthetic mixtures dissolved in milli-Q water (10 μg/mL) were run on an Agilent HP1100 chromatographic system (Hewlett Packard, Palo Alto, CA, USA) controlled by Chemstation version B.0.03. The chromatographic system was coupled to an Agilent XCT ion trap equipped with an electrospray ionization (ESI) source operated in positive ion mode.

HPLC separations were carried out using a Zorbax Eclipse C8 column (4.6 mm i.d. × 150 mm, 5 μm) maintained at 25°C, at a flow rate of 0.75 mL min^{-1} with a gradient of 0.05% (v/v) heptafluorobutyric acid (HFBA) in water (solvent A) and 0.05% (v/v) HFBA in acetonitrile (solvent B). The solvent program was as follows: the gradient ramped from 0 to 80% B in 60 min and was held until 63 min. The column was then returned to the initial conditions and re-equilibrated until 73 min.

LC/MS settings were as follows: capillary voltage 3500 V, nebulizer gas (N_2) pressure 60 psi, drying gas (N_2) flow 11 L/min, drying temperature 350°C. The mass spectrometer scanned from 50–2000 *m/z*. LC/MS conditions were optimized to produce positive molecular ions $[M+H]^+$ via ESI at atmospheric pressure. Several cone voltages from 20 to 120 V

were tested by repeat injections of LCPA standards (see Fig. S1, Supporting Information). A cone voltage of 20 V was found to produce the most efficient formation of $[M+H]^+$ ions and was used for all subsequent analyses. Fragmentation experiments (MS^n) were performed using a fragmentation voltage of 1.00 V.

RESULTS AND DISCUSSION

HPLC separation and mass spectral identification of long-chain polyamine synthetic standards

LCPA chromatographic separation

We used ion-pairing reversed-phase liquid chromatography (RPLC) to increase the hydrophobicity and therefore the chromatographic retention of LCPAs. By adding 3.8 mM heptafluorobutyrate (0.05% vol) in the mobile phases and optimizing the gradient solvent conditions, chromatographic separation of individual LCPAs was obtained for the two LCPA standard mixtures analyzed in this study (Tables 1 and 2, Figs. 1 and 3). In our previous study,[13] a Zorbax Eclipse XDB C18 column (4.6 mm i.d. × 150 mm, 5 μm) was used and the mobile phases A and B were fortified with 0.1% (v/v) HFBA. In this study, the gradient was optimized for high resolution of underivatized aliphatic LCPAs and a Zorbax Eclipse C_8 column (4.6 mm i.d. × 150 mm, 5 μm) was found to achieve better chromatographic separation compared to the C_{18}.

The use of ion-pairing reagents (such as HFBA) with ESI-MS is known to cause signal suppression for basic compounds, due to their ability to form gas-phase ion pairs with positively charged analytes.[21,22] Propionic acid can be used to counterbalance ion suppression.[18] However, we did not observe significant LCPA signal enhancement with the addition of propionic acid to our mobile phase so we did not use it.

Natural polyamines that are involved in silicic acid precipitation display variable degrees of methylation and chain length. We used two standard mixtures of aliphatic

Table 1. Retention times and peak identification (*m/z* of the singly $[M+H]^+$ and doubly $[M+2H]^{2+}$ charged ions with their relative abundances, normalized to base peak) of synthetic aliphatic non-methylated long-chain polyamine standard mixture A (see chromatogram in Fig. 2)

Peak #	RT (min)	ID $[M+H]^+$	ID $[M+2H]^{2+}$	n	R =	Peak #	RT (min)	ID $[M+H]^+$	ID $[M+2H]^{2+}$	n	R =
1	35.9	304.5 *(100)*	–	4	-H	**13**	36.0	318.5 *(100)*	–	4	$-CH_3$
2	37.6	361.5 *(100)*	181.2 *(1.0)*	5	-H	**14**	37.7	375.5 *(100)*	188.3 *(1.2)*	5	$-CH_3$
3	38.8	418.6 *(100)*	209.7 *(2.3)*	6	-H	**15**	39.0	432.6 *(100)*	216.7 *(2.7)*	6	$-CH_3$
4	40.0	475.6 *(100)*	238.3 *(3.0)*	7	-H	**16**	40.1	489.6 *(100)*	245.4 *(3.8)*	7	$-CH_3$
5	40.8	532.6 *(100)*	266.8 *(4.3)*	8	-H	**17**	41.0	546.6 *(100)*	274.0 *(4.4)*	8	$-CH_3$
6	41.4	589.7 *(100)*	295.4 *(6.0)*	9	-H	**18**	41.9	603.7 *(100)*	302.4 *(9.3)*	9	$-CH_3$
7	42.1	646.7 *(100)*	323.9 *(11.5)*	10	-H	**19**	42.5	660.7 *(100)*	331.2 *(19.6)*	10	$-CH_3$
8	42.9	703.8 *(100)*	352.8 *(33.2)*	11	-H	**20**	43.0	717.8 *(100)*	359.7 *(39.1)*	11	$-CH_3$
9	43.5	760.9 *(100)*	381.3 *(88.5)*	12	-H	**21**	43.6	774.9 *(91.3)*	388.3 *(100)*	12	$-CH_3$
10	44.0	818.0 *(30)*	409.9 *(100)*	13	-H	**22**	44.1	832.0 *(30.4)*	416.9 *(100)*	13	$-CH_3$
11	44.5	875.0 *(15.0)*	438.3 *(100)*	14	-H	**23**	44.6	889.0 *(10.2)*	445.4 *(100)*	14	$-CH_3$
12	45.2	932.0 *(7.2)*	465.9 *(100)*	15	-H	**24**	45.3	946.0 *(5.1)*	473.9 *(100)*	15	$-CH_3$

Table 2. Retention times and peak identification (*m/z* of the singly $[M+H]^+$; doubly $[M+2H]^{2+}$; triply $[M+3H]^{3+}$; and quadruply $[M+4H]^{4+}$ charged ions with their relative abundances, normalized to base peak) of synthetic aliphatic methylated long-chain polyamine standard mixture B (see chromatogram in Fig. 3)

Peak #	RT (min)	Peak identification $[M+H]^+$	Peak identification $[M+2H]^{2+}$	Peak identification $[M+3H]^{3+}$	Peak identification $[M+4H]^{4+}$	n
1′	25.4	245.3 *(100)*	–	–	–	2
2′	27.0	316.4 *(100)*	–	–	–	3
3′	27.9	387.5 *(100)*	194.3 *(2.4)*	–	–	4
4′	29.2	458.6 *(100)*	229.8 *(4.5)*	–	–	5
5′	29.8	529.7 *(100)*	265.4 *(5.5)*	–	–	6
6′	30.2	600.7 *(100)*	301.1 *(8.5)*	–	–	7
7′	31.1	671.8 *(100)*	336.6 *(28.0)*	224.6 *(0.6)*	–	8
8′	31.5	742.9 *(100)*	372.1 *(31.9)*	248.4 *(2.1)*	–	9
9′	31.7	814.0 *(100)*	407.7 *(50.5)*	272.2 *(9.2)*	–	10
10′	32.9	885.1 *(50.8)*	443.3 *(100)*	295.8 *(3.9)*	220.9 *(0.3)*	11
11′	35.4	956.2 *(27.0)*	478.8 *(100)*	319.7 *(11.1)*	239.9 *(0.4)*	12
12′	37.8	1027.3 *(14.5)*	514.4 *(100)*	343.3 *(12.5)*	257.3 *(0.8)*	13

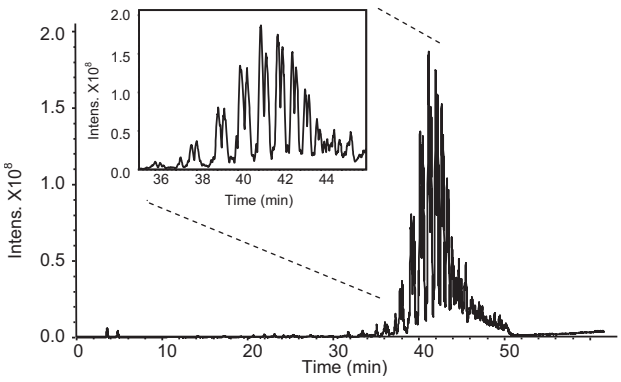

Figure 1. LC/ESI-MS base peak chromatogram of a mixture of non-methylated linear polypropyleneimine standards (LCPA mixture A). The top insert shows a close-up of the LCPA elution time window (RT = 36–46 min).

non-methylated (standard mixture A) and methylated (standard mixture B) polypropylamines that are similar to the polyamine structural moieties identified in various diatoms and sponge species.[8,10] Standard mixture A consists of a series of 24 linear polypropyleneimine compounds varying in their number of propylamine repeat units

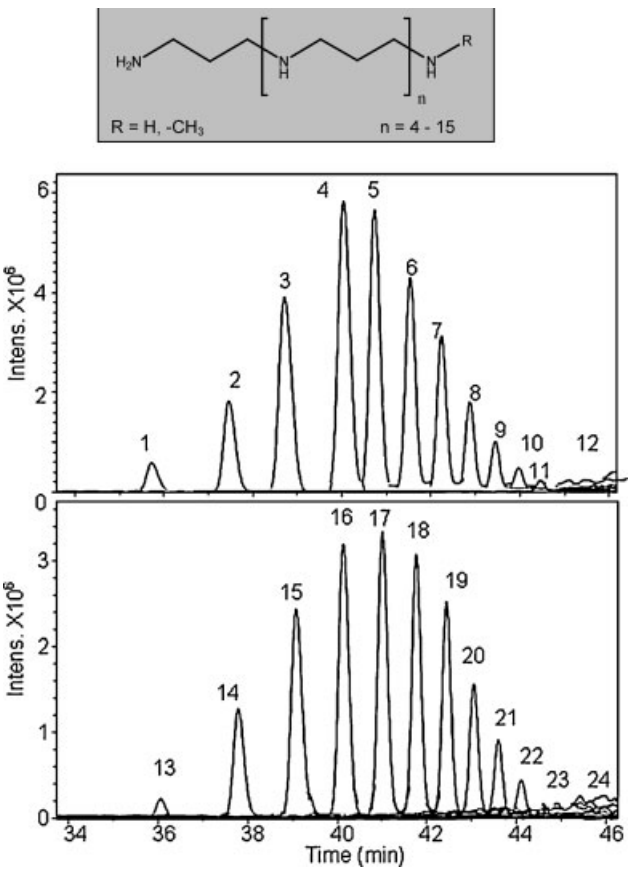

Figure 2. Overlapped LC/ESI-MS extracted ion chromatograms of LCPA standard mixture A, containing non-methylated LCPAs (peaks 1–12, n = 4–15; R = H) and partially methylated LCPAs (peaks 13–24, n = 4–15; R = -CH_3). The top shaded inset displays the general structure of the compounds present in the mixture. Refer to Table 1 for peak assignments.

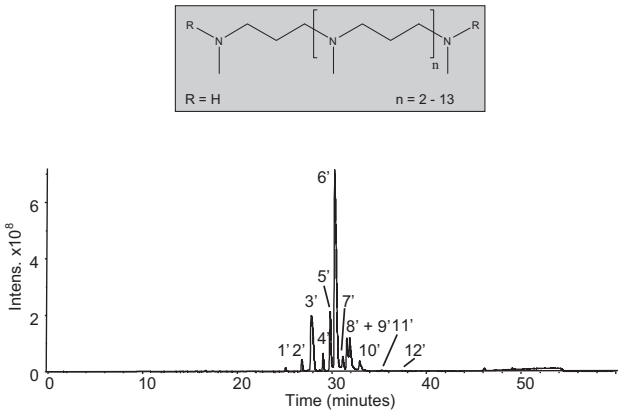

Figure 3. LC/ESI-MS base peak chromatogram of a mixture of methylated, linear polypropyleneimine standards (LCPA mixture B). The top shaded inset displays the general structure of the compounds present in the mixture. Refer to Table 2 for peak assignment.

(n = 4–15) and in the presence or absence of a terminal methyl group (R = -H, -CH_3; Fig. 2). All 24 LCPAs from standard mixture A elute between 35 and 45 min (Fig. 2), according to their carbon chain length and degree of terminal methylation. LCPAs varying in their number of N-propylamine repeat units are all baseline separated with each additional N-propylamine resulting in a longer retention time (peaks 1–12 and 13–24, Table 2 and Fig. 3). LCPAs with the same number (n) of propylamine repeat units but with different degrees of terminal methylation (R = -H or -CH_3) elute in peaks that are not completely resolved (Fig. 1). The LCPA standard mixture B consists of a series of 12 methylated polypropyleneimine compounds whose structures only differ by the number of N-methylpropylamine repeats (n = 2–13; Fig. 3). Most compounds in this mixture are also baseline separated under the chromatographic conditions employed, except for peaks 8′ and 9′ (n = 9 and 10). A log-log plot of LCPA retention time versus the number of propylamine units (n) has a strong positive linear correlation ($r > 0.99$) on a C_8 reversed-phase column for both non-methylated (R = -H) and partially methylated (R = -CH_3) long-chain polyamines of the standard mixture (Fig. 4). Such a plot could be used to develop an HPLC-based LCPA retention index that should be helpful in identifying unknown aliphatic LCPAs of varying chain length from environmental samples.

Mass spectrometric analysis

Due to the relatively high pKa values of the amines in LCPAs, they carry multiple positive charges in a wide range of pHs.[17] Therefore, LC/MS analysis was carried out in the positive ionization mode. Attempts to form deprotonated molecules via negative ESI were not successful. Each LCPA formed abundant protonated species ($[M+H]^+$) with no other adducts (Fig. 5) as well as a relatively low abundance of doubly charged $[M+2H]^{2+}$ ions. The abundance of doubly charged $[M+2H]^{2+}$ ions increased with LCPA chain length (Table 2) much like peptides and proteins, probably due to the higher number of nitrogen atoms available for protonation. Multiply charged LCPAs have not been previously reported, in part because it is not possible to detect those ions

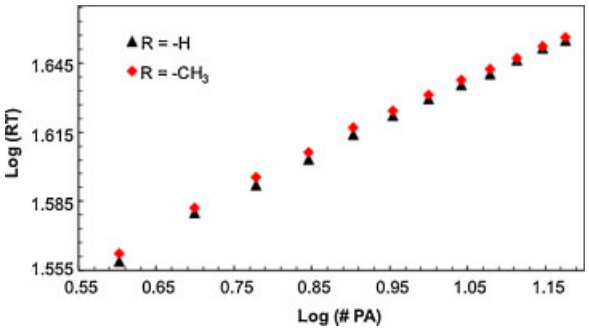

Figure 4. Log-log plot of retention times (RT, in minutes) versus number of propylamine repeat units (#PA) for non-methylated (R = -H) and partially methylated (R = -CH_3) long-chain polyamines from the standard mixture A (see general structure in Fig. 2).

without chromatographic separation due to the complex nature of the natural LCPA mixtures.

The mass spectra of peak 4 shows an abundant protonated $[M+H]^+$ (*m/z* 475.6; 100% relative intensity) followed by an ion at *m/z* 238.3 (3.0% relative intensity) corresponding to the doubly charged $[M+2H]^{2+}$ ion (Table 1 and Fig. 5). Analogous observations can be made from the mass spectra of LCPAs of standard mixture B. The mass spectrum of peak 6′ shows an abundant $[M+H]^+$ ion at *m/z* 600.7 followed by a relatively less abundant ion at *m/z* 301.1 (8.5% relative intensity), also corresponding to the $[M+2H]^{2+}$ ion (Table 2 and Fig. 6). Similarly, the mass spectrum of peak 9′ displays an abundant peak at *m/z* 814.0 ($[M+H]^+$) followed by two abundant peaks at *m/z* 407.7 ($[M+2H]^{2+}$; 50.5% relative intensity) and 272.2 ($[M+3H]^{3+}$; 9.2% relative intensity). Increasing LCPA chain length (and therefore molecular weight) correlates with the relative abundance of ions corresponding to various protonation states ($[M+2H]^{2+}$, $[M+3H]^{3+}$ and $[M+4H]^{4+}$). The mass spectrum of peak 12′ illustrates this trend, where the most abundant ion corresponds to the doubly charged species observed at *m/z* 514.4 ($[M+2H]^{2+}$; 100% relative intensity), followed by *m/z* 1027.3 ($[M+H]^+$; 14.5% relative intensity), *m/z* 343.3 ($[M+3H]^{3+}$; 12.5% relative intensity) and *m/z* 257.3 ($[M+4H]^{4+}$; 0.8% relative intensity) (Table 2 and Fig. 6). In general, for LCPAs having $m/z < 900$, the most abundant ion corresponds to the singly charged ($z = 1$), protonated molecular ion, whereas for LCPAs having $m/z > 900$, the most intense peak in the mass spectra corresponds to the $[M+2H]^{2+}$ ion. In some cases ($m/z > 1200$), the $[M+H]^+$ ion can hardly be detected in the mass spectra.

Product ion spectral data from $[M+H]^+$

LCPA mass spectral fragmentation patterns, as obtained by collision-induced dissociation of protonated molecular ions $[M+H]^+$, exhibited many characteristic and repetitive features, as rationalized in Schemes 1(A)–1(C).

The product ion spectrum of selected non-methylated LCPA species (LCPA peak #6) from standard mixture A (Fig. 7(A)) shows two series of mass fragments shifted by 17 Da, corresponding to the loss of the terminal ammonia (e.g. *m/z* 343.5 and 360.4; Schemes 1(A) and 2). Molecular species from each series are further separated by 57 Da (e.g. *m/z* 286.5 and 343.5), resulting from losses of N-propyleneimine units (-$C_3H_7N_1$; Scheme 1(A)). This over-

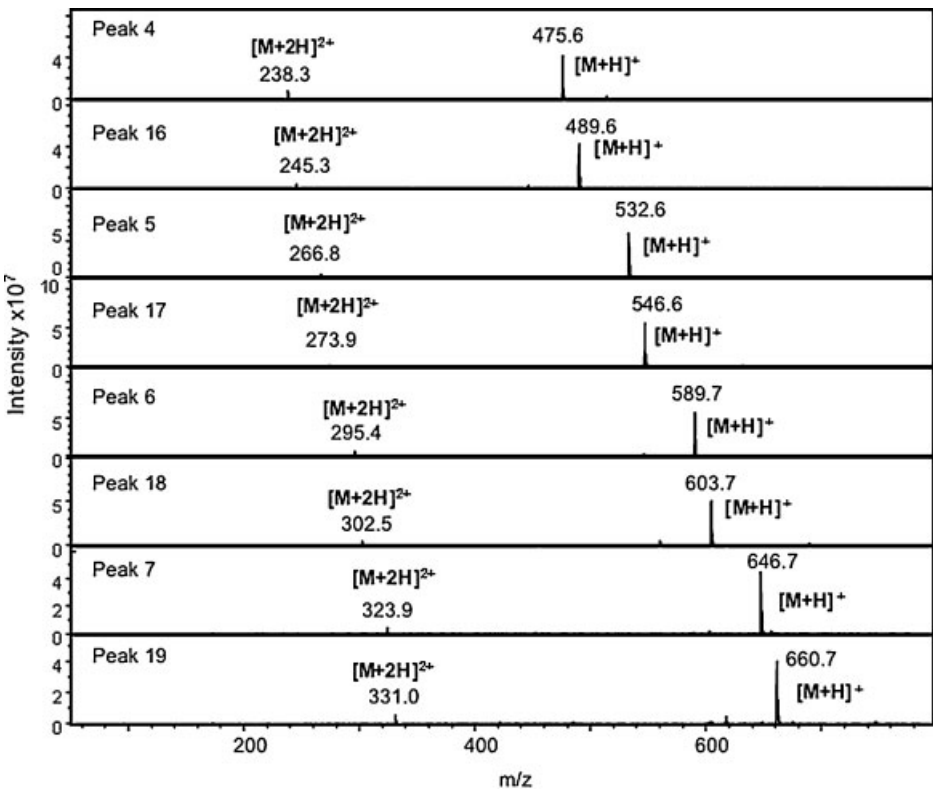

Figure 5. LC/ESI-MS spectra of selected LCPAs from standard mixture A (see chromatogram in Fig. 2).

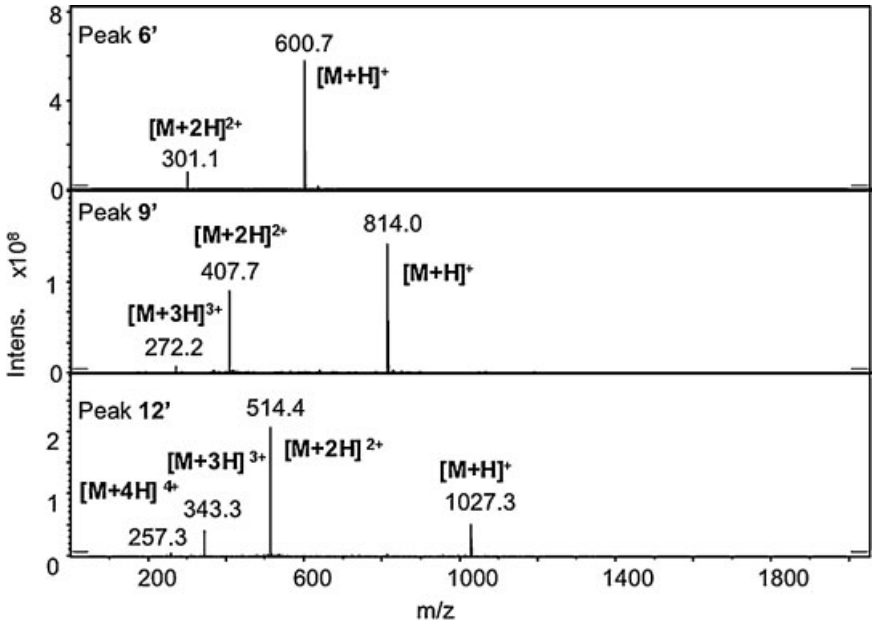

Figure 6. LC/ESI-MS spectra of selected LCPAs from standard mixture B (see chromatogram in Fig. 3).

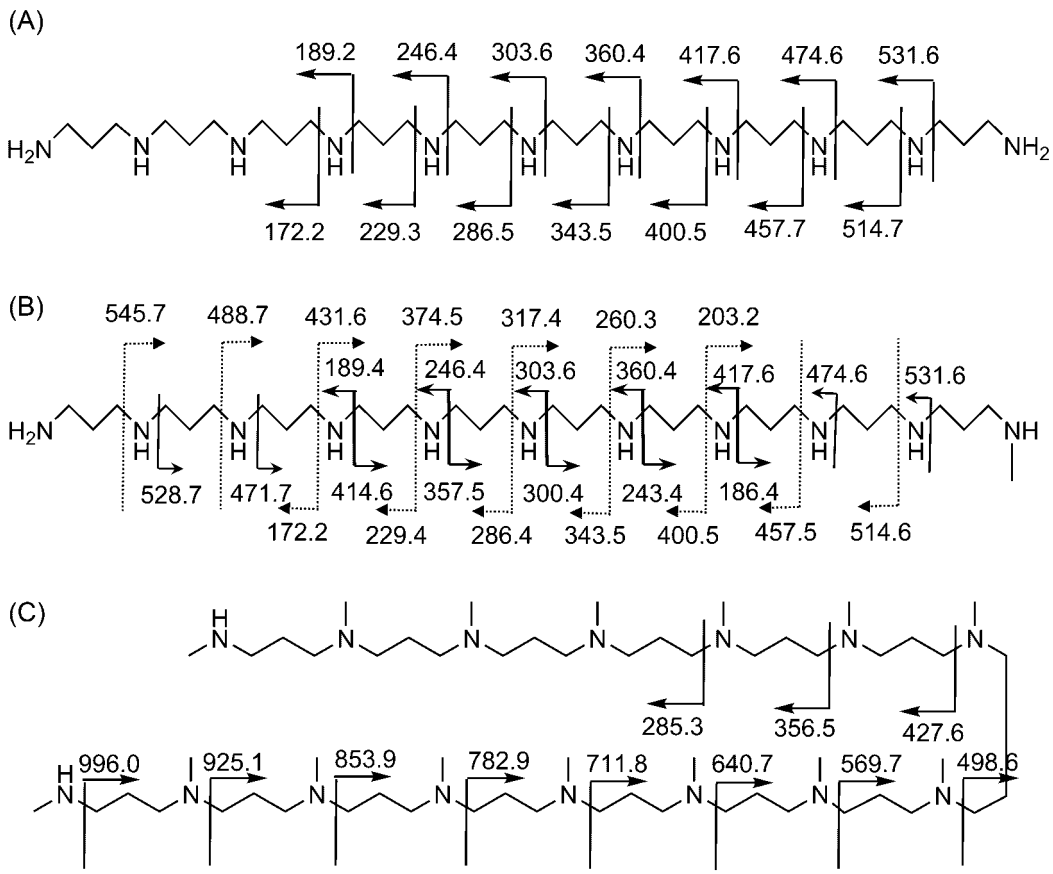

Scheme 1. Proposed fragmentation patterns observed in ESI mass spectra of (A) LCPA standard mixture A, peak # 6 (see Fig. 7(A) for MS/MS spectra); (B) LCPA standard mixture A, peak # 18 (see Fig. 8(A) for MS/MS spectra); and (C) LCPA standard mixture B, peak # 12′ (see Fig. 9(A) for MS/MS spectra). The cleavage positions leading to the respective product ion spectra in Figs. 7(A), 8(A) and 9(A) are depicted by arrows, and the corresponding molecular masses are indicated.

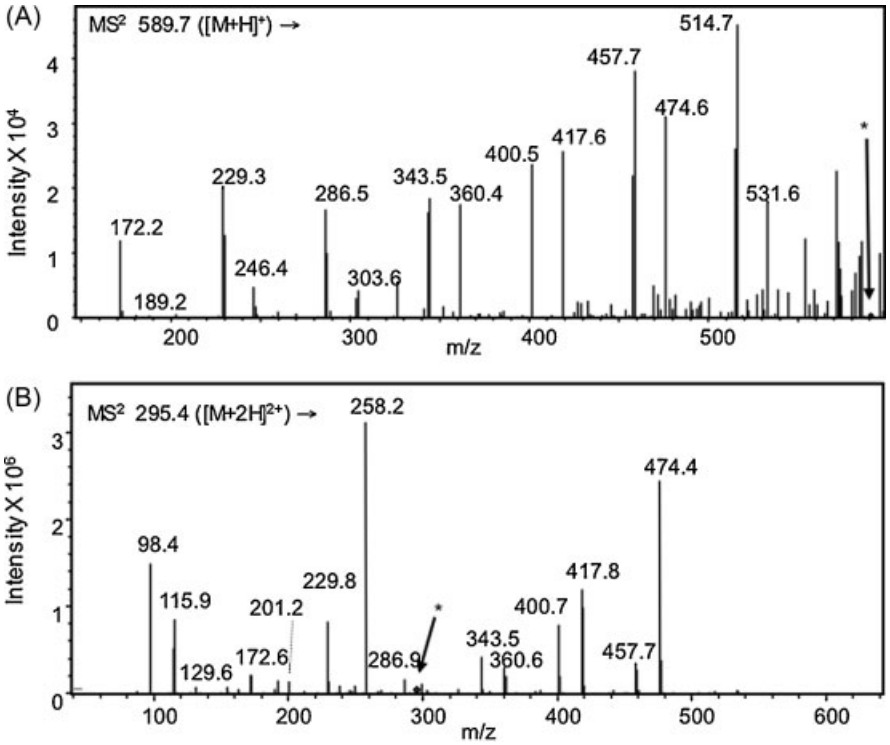

Figure 7. LC/ESI-MS/MS product ion mass spectra of the protonated singly (A) and doubly (B) charged molecular ion of LCPA peak # 6 (LCPA standard mixture A; *m/z* 588.7).

all pattern indicates that several mechanisms are operating simultaneously at the site of positively charged nitrogen atoms and that fragmentation of the aliphatic chain occurs at both sides of the positively charged nitrogen in secondary amine groups, confirming previous observations.[15] After cleavage of the C–N bond, one or two different fragments can be formed, as rationalized in Scheme 2. In this example, the secondary amine located next to the protonated nitrogen atom allows for internal proton transfer, resulting in the detection of a positively charged N-terminated fragment (*m/z* 360.4; Scheme 2). The fragment ion observed at *m/z* 343.5 is likely formed by the expulsion of ammonia (17 Da) from *m/z* 360.4, followed by rearrangement in a ring structure, as previously observed for putrescine[23,24] and for acylpoly-

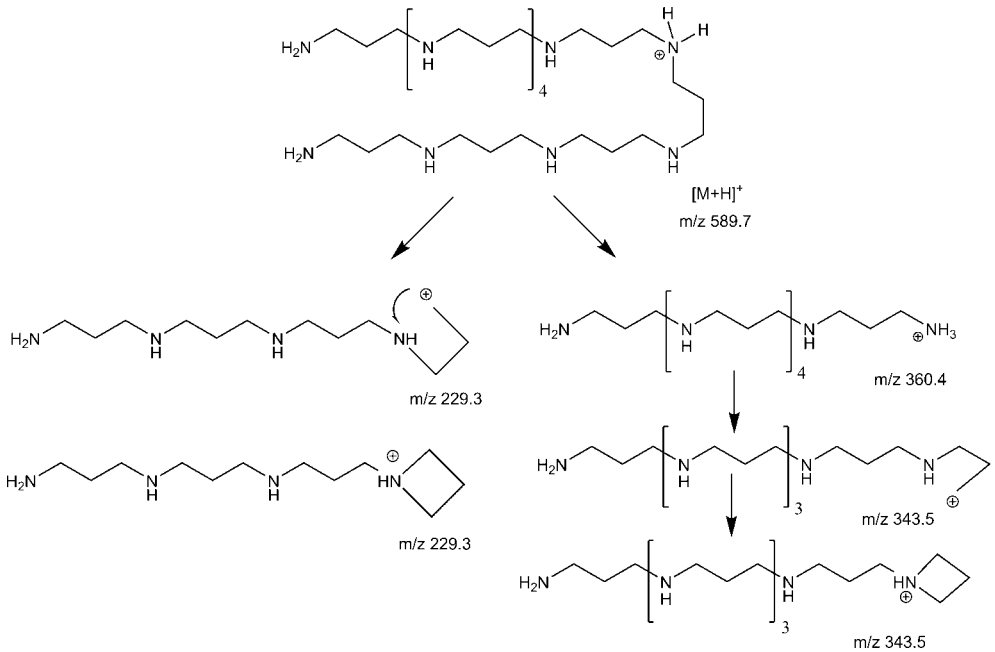

Scheme 2. General fragmentation pathways of LCPAs from standard mixture A (i.e. LCPA peak # 6; see Scheme 1(A)), leading to the formation of product ions: *m/z* 343.5 and *m/z* 229.3, formed by internal proton transfer from a secondary amine group leading to a positively charged N-terminal fragment, with subsequent loss of ammonia and ring formation.

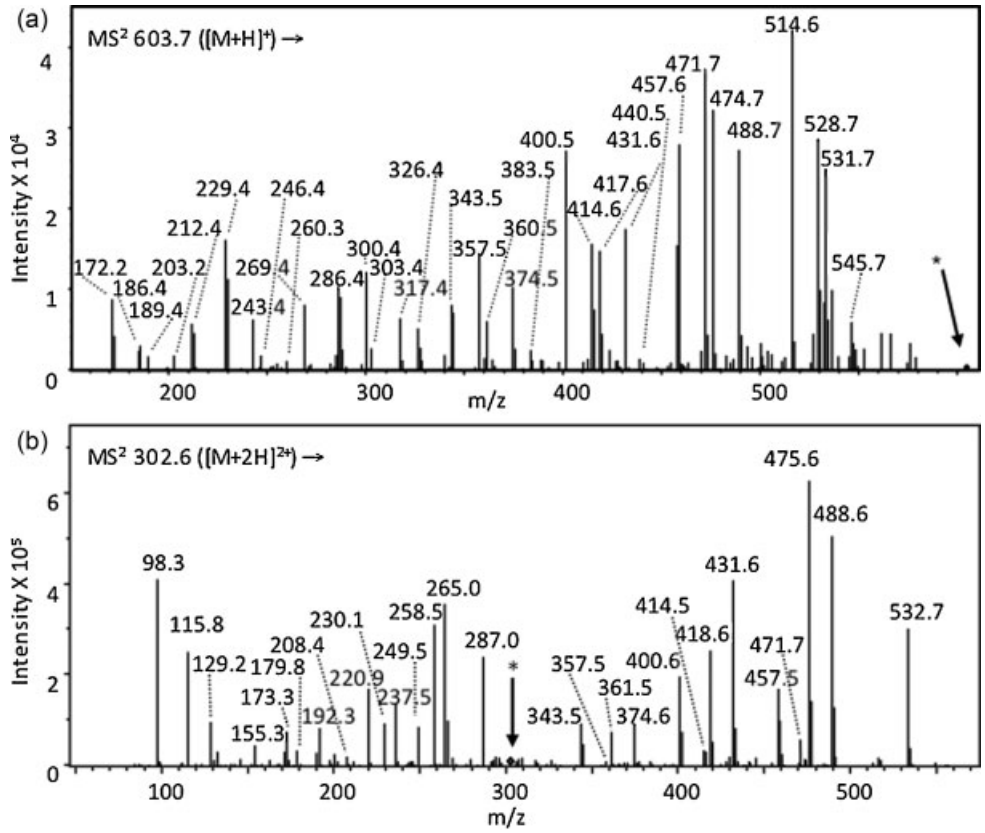

Figure 8. LC/ESI-MS/MS product ion mass spectra of the protonated singly (A) and doubly (B) charged molecular ion of LCPA peak # 18 (LCPA standard mixture A; *m/z* 602.7).

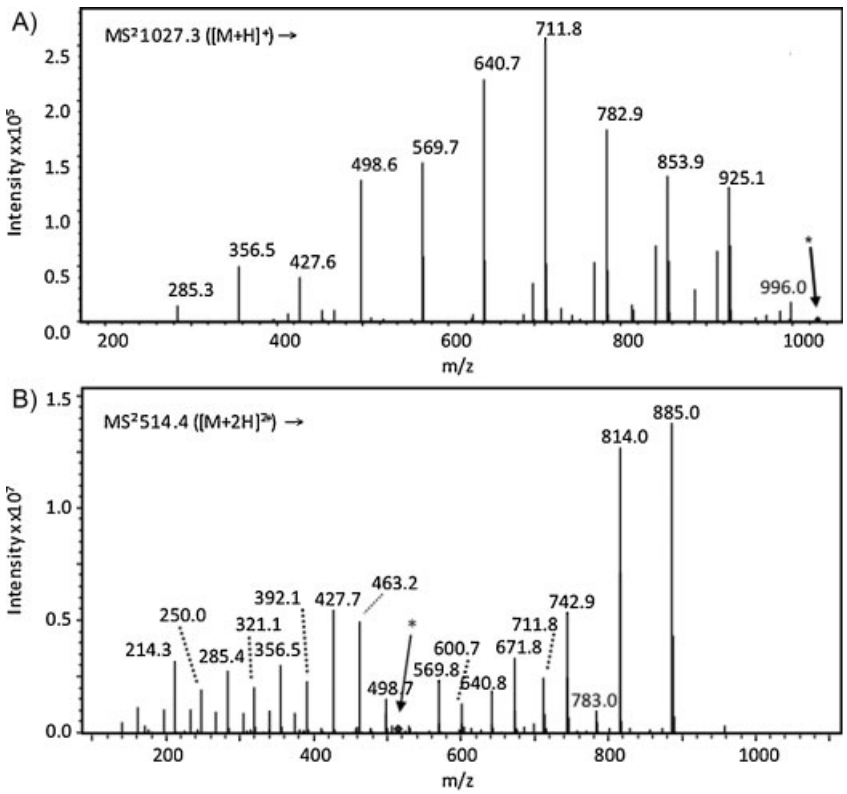

Figure 9. LC/ESI-MS/MS product ion mass spectra of the protonated singly (A) and doubly (B) charged molecular ion of LCPA peak # 12′ (LCPA standard mixture B; *m/z* 1026.3).

amines.[25,26] All product ions observed in the MS^2 spectra of LCPA peak 6 (Fig. 7(A)) are listed and rationalized in Table S1 (see Supporting Information).

Similar fragmentation patterns are also observed for all other non-methylated LCPAs from standard mixture A (peaks 1–12 in Fig. 2; n = 4–15 and R = -H), regardless of chain length. However, partial methylation of the terminal primary amine group (standard mixture A, peaks 13–24 in Fig. 3 and R = -CH_3) increases the complexity of the product ion mass spectra. The product ion mass spectra of the protonated singly charged molecular ion of LCPA peak #18 is displayed in Figure 8(A). Also, a few of the abundant product ions observed in the MS^2 spectra of LCPA peak 18 (Fig. 8(A)) are listed and rationalized in Table S1 (see Supporting Information). Most fragments can again be attributed to a cleavage at both sides of the secondary amine group, as shown by the arrows in the structure (Scheme 1(B)). However, another set of new fragments observed at *m/z* 212.4; 269.4; 326.4 and 383.5 cannot be explained by simple cleavage at the C–N bond alone. Those ions may result from gas-phase fragmentation and/or rearrangement in the trap.

Fragmentation of the fully methylated LCPAs from standard mixture B produced a much simpler product ion mass spectra (Fig. 9(A)) dominated by neutral losses of 71 Da, corresponding to *N*-methylpropylamine repeat units (-$C_4H_9N_1$) (e.g. 640.7 and 711.8; Scheme 1(C)). Analogous fragmentation was observed for all other methylated LCPAs from standard mixture B (peaks 1′–12′ in Fig. 3; n = 2–13), regardless of chain length. Methylated aliphatic long-chain polyamines fragment preferentially at the C–N bond of a positively charged nitrogen atom as rationalized by Scheme 3. If the amine group located next to the positively charged nitrogen is tertiary, then only the C-terminal fragment bears a positive charge (Scheme 3).

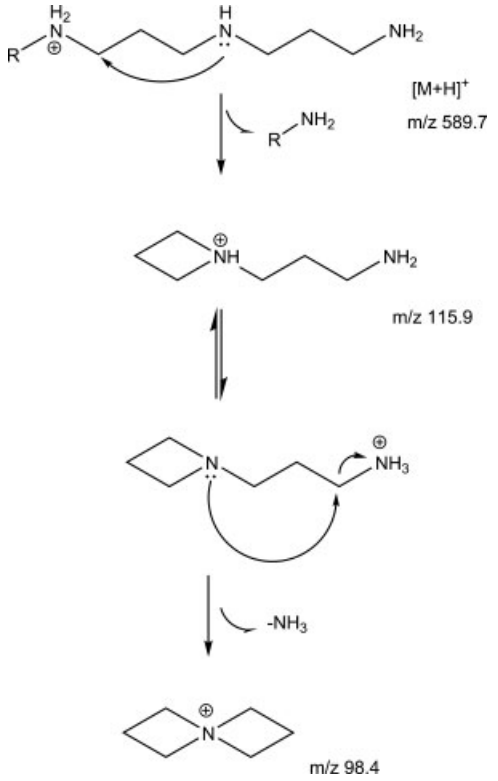

Scheme 4. Mass spectral fragmentation of the terminal part of the $[M+2H]^{2+}$ ions of the non-methylated LCPA standards 1–24.

Product ion spectra from $[M+2H]^{2+}$

Since the doubly charged ions $[M+2H]^{2+}$ are abundant in the LCPA mass spectra, MS/MS fragmentation of these diprotonated ions was also studied. The ESI tandem mass spectra of $[M+2H]^{2+}$ ions of LCPA #6 (*m/z* 295.4) and #18 (*m/z* 302.6) are shown in Figs. 7(B) and 8(B). The most abundant ion observed in the tandem mass spectrum of the $[M+2H]^{2+}$ ion of LCPA peak #6 was observed at *m/z* 258.2 (Fig. 7(B)) and corresponds to the doubly charged ion $[M+2H–C_3H_9N_2]^{2+}$ (Table S2, Supporting Information). Fragmentation of the $[M+2H]^{2+}$ ion (*m/z* 295.4) produces similar fragments as those described previously for the singly charged $[M+H]^+$ ion (same neutral losses). A suite of doubly charged fragments separated by 28.5 Da (half the mass of

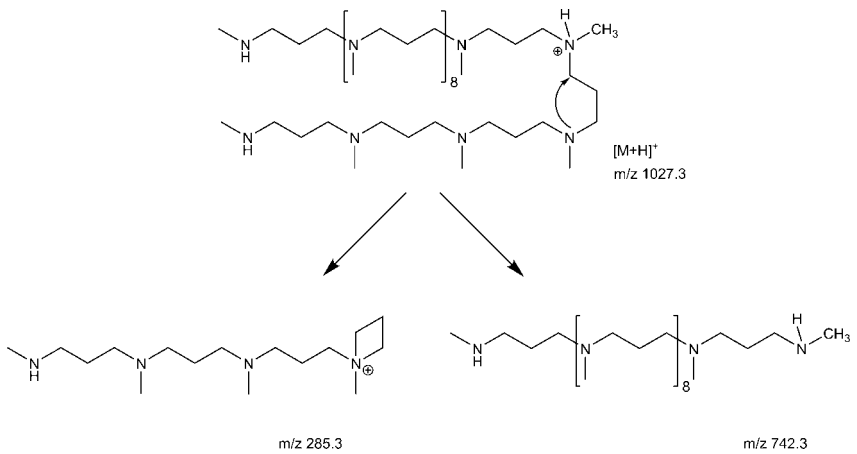

Scheme 3. General fragmentation pathways of LCPAs from standard mixture B (i.e. LCPA peak # 12′ see Scheme 1(C)), leading to the formation of selected daughter ion *m/z* 285.3. After C–N bond cleavage, only the C-terminated fragment bears a positive charge and can be detected.

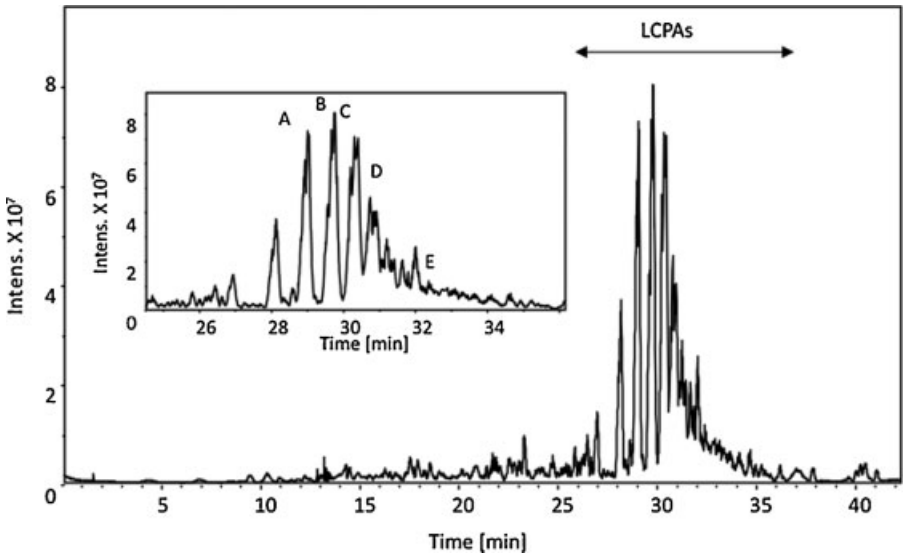

Figure 10. LC/ESI-MS base peak chromatogram of a HF extract of cleaned sedimentary diatoms from sediment core TNO57-13PC4 (799–801 cm; ~17 000 years). The top insert shows a close-up of the LCPA elution time window (RT = 24–36 min).

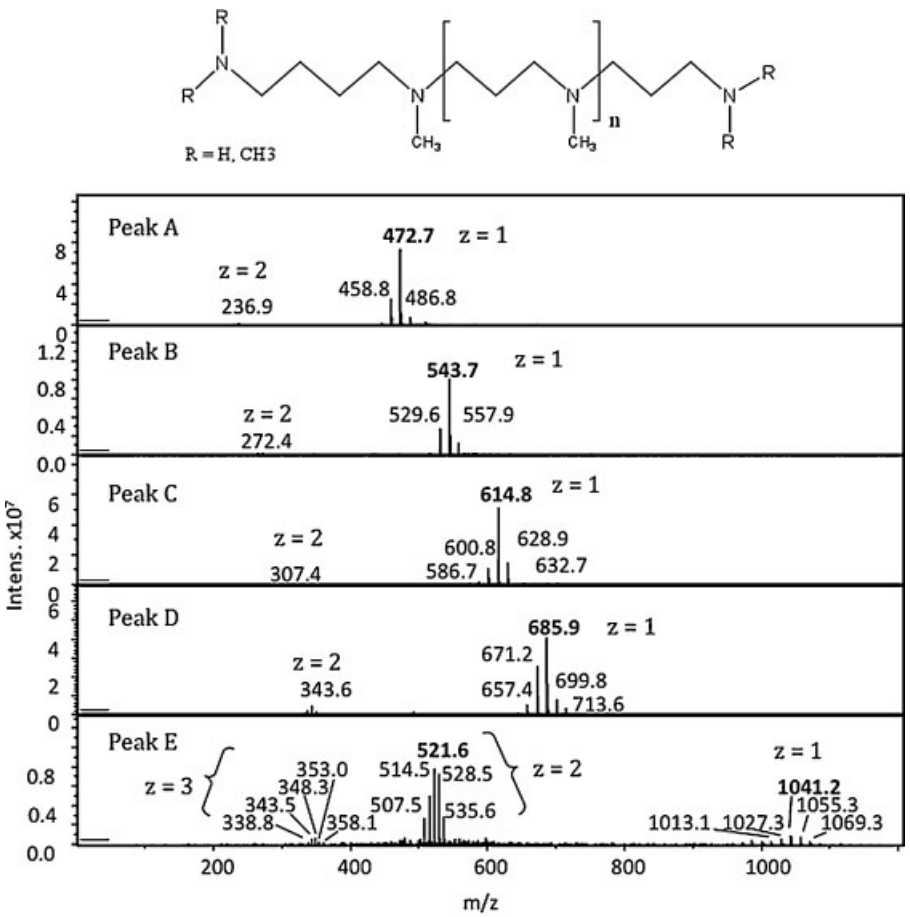

Figure 11. LC/ESI-MS spectra of selected putrescine based *N*-methylpropylamine LCPAs from sediment core TNO57-13PC4 (799–801 cm), showing the singly charged (z = 1), doubly charged (z = 2) and triply charged (z = 3) species. The generic structure of these putrescine-based LCPAs is shown on the top.

N-propyleneimine neutral losses, $C_3H_7N_1$) is also detected in the tandem MS spectrum of peak #6, at *m/z* 229.8 ($[M+2H–C_6H_{16}N_3]^{2+}$); *m/z* 201.2 ($[M+2H–C_9H_{22}N_3]^{2+}$) and *m/z* 172.6 ($[M+2H–C_{12}H_{29}N_4]^{2+}$) (Table S2, Supporting Information). Singly charged ions are also observed in the MS/MS spectra of the $[M+2H]^{2+}$ ion. These ions correspond to the carbon–nitrogen cleavage shown by arrows in Scheme 1(A) and result from neutral losses of various propylamine units (e.g. *m/z* 474.4 $[LCPA–C_6N_2H_{15}]^{2+}$, 417.8 $[LCPA–C_9N_3H_{22}]^{2+}$, 360.6 $[LCPA–C_{12}N_4H_{29}]^{2+}$) (Table S2, Supporting Information).

In the tandem mass spectra of the $[M+2H]^{2+}$ ion of all non-methylated LCPAs from standard mixtures A and B (peaks 1–24), the low molecular weight fragments observed at *m/z* 98.3 and 115.9 had relatively high abundance (Figs. 7(B) and 8(B)). Formation of these two fragments can be rationalized by Scheme 4, as observed in the MS/MS spectra of acylpolyamines.[26]

The ESI tandem mass spectra corresponding to the doubly charged $[M+2H]^{2+}$ ion of LCPA peak 12′ (*m/z* 514.4) is shown in Fig. 9(B). This spectra displays the same suite of singly charged ions, separated by 71 Da (corresponding to *N*-methylpropylamine neutral losses; at *m/z* 285.4; 356.5; 427.6; 498.6; 569.7; ...), as observed in the MS spectra in Fig. 9(A); as well as a series of doubly charged ions separated by 35.5 Da (half the mass of *N*-methylpropylamine neutral loss, $C_4H_9N_1$) observed at *m/z* 214.3, 250.0, 285.4, 321.1, 356.5, 392.1, 427.7, 463.2 and 498.7 (Table S4, Supporting Information).

HPLC separation and MS identification of long-chain polyamines extracted from sediments

Separation of natural polyamines in complex samples requires high resolution because of the large number of components present and the large range of polarities encountered among those mixtures. In previous studies, we reported the presence of a series of LCPAs from a diatom rich sediment core originating from the Atlantic sector of the Southern Ocean.[12,13] However, all LCPAs eluted in one broad chromatographic peak, complicating interpretation of the data. The chromatogram of the same sediment extract (TNO5713, 799–801 cm),[13] run using our new method, clearly shows a dramatic improvement in the chromatographic separation of individual LCPA components of the mixture (Fig. 10). However, individual LCPAs are not all baseline separated, due to their more complex distribution in natural samples compared to the synthetic standard LCPA mixtures used to optimize the method. In fact, each chromatographic peak in Fig. 10 represents a series of three to five N-methylated propylamine units. The mass spectra of selected peaks A–E (Fig. 10) are displayed in Fig. 11. Peaks A and B consist of mixtures of three N-methylated propyleneimine units, each. LCPA species in peak A (*m/z* 458.8, 472.7 and 486.8) have the same number (n = 4) of *N*-methylpropylamine repeat units but vary in their degree of methylation, R (see structure in Fig. 11). LCPA species in peak B (*m/z* 529.6, 543.7 and 557.9) have n = 5 *N*-methylpropylamine repeat units and also vary in their degree of methylation, R (see structure in Fig. 11). Peaks C, D and E consist of mixtures of five N-methylated propyleneimine units each. LCPA species in peak C (*m/z* 586.7, 600.3 614.8, 628.9 and 632.7) have n = 6 *N*-methylpropylamine repeat units, while LCPAs in peaks D (*m/z* 657.4, 671.2, 685.9, 699.8 and 713.6) and E (*m/z* 1013.1, 1027.3, 1041.2, 1055.3 and 1069.3) have n = 7 and n = 12 *N*-methylpropylamine repeat units, respectively, with 5 different degrees of methylation R. Similar to the synthetic standards, the ESI mass spectra of natural LCPAs display a small doubly charged $[M+2H]^{2+}$ ion (z = 2) whose intensity increases with increasing LCPA chain length (Fig. 11). The mass spectrum of the LCPA mixture in peak E (Fig. 11) shows that the doubly charged $[M+2H]^{2+}$ ions (*m/z* 507.5, 514.5, 521.5, 528.5 and 535.5) are the most abundant ions, and that the intensity of the triply charged $[M+3H]^{3+}$ ions is about the same as for the molecular ions $[M+H]^+$. The pseudomolecular ions $[M+H]^+$ of natural LCPAs whose molecular weight is above 900 decrease in intensity and almost disappear with a concomitant increase in intensity of the $[M+2H]^{2+}$ and $[M+3H]^{3+}$ ions, as observed with the synthetic LCPA standard mixtures.

CONCLUSIONS

Here we describe the chromatographic separation and structural characterization by ion-pairing reversed-phase HPLC tandem mass spectrometry (MS^2) of 36 aliphatic, propylamine- and *N*-methylpropylamine-based synthetic LCPA standards that are analogous to the polyamines found in diatom frustules and sponge spicules.

LCPAs were detected by electrospray ionization mass spectrometry (ESI-MS) as singly $[M+H]^+$ and multiply $[M+nH]^{n+}$ charged protonated ions. The abundance of $[M+nH]^n$ increased linearly as a function of LCPA chain length (n), with a concomitant disappearance of $[M+H]^+$. The formation of multiply charged species has not been observed previously during analysis of LCPA mixtures. This significantly increases the complexity of the MS spectra, justifying the need for good chromatographic separation of complex LCPA mixtures.

Tandem mass spectrometry (MS/MS) fragmentation of the $[M+H]^+$ of propylamine-based LCPAs produced a series of ions separated by 57 Da ($[M+H–C_3H_8N_1]^+$, $[M+H–C_6H_{15}N_2]^+$, $([M+H–C_9H_{22}N_3]^+$; ...), corresponding to losses of propylamine groups ($C_3H_7N_1$), whereas the fragmentation of the $[M+H]^+$ ion of *N*-methylpropylamine LCPAs produced a series of ions separated by 71 Da ($[M+2H–C_1H_4N_1]^+$, $[M+2H–C_5H_{13}N_2]^+$, $[M+2H–C_9H_{22}N_3]^+$, ...) due to neutral losses of *N*-methylpropylamine units ($C_4H_9N_1$).

Fragmentation of the $[M+2H]^{2+}$ ion of propylamine LCPAs produced a series of doubly charged fragment ions $[M+2H–(C_3H_9N_2)_n]^{2+}$ as well as the common singly charged ions separated by 57 Da whereas fragmentation of the $[M+2H]^{2+}$ ion of *N*-methylpropylamine LCPAs leads mainly to the doubly charged ions ($[M+2H–C_1H_4N_1]^{2+}$, $[M+2H–C_5H_{13}N_2]^{2+}$, ...) and an unusual series of singly charged species ($[M+H–C_{10}H_{25}N_4]^+$, $[M+H–C_{14}H_{34}N_5]^+$, $[M+H–C_{18}H_{43}N_6]^+$, ...).

This LC/ESI-MS method was then used to separate LCPAs extracted from a diatom-rich sediment core originating from the Southern Ocean and showed a dramatic improvement in

the chromatographic separation of the various natural LCPA species present in the sediment extract.

The results show that our LC/ESI-MS method can be a powerful tool for the characterization of long-chain polyamines without complex biochemical isolation and purification steps (ion exchange, size exclusion, dialysis). This new method can be used to identify and eventually quantify complex mixtures of LCPAs, which was not possible before. Also, improved separation of LCPAs now allows for their purification in natural samples for studies of silica precipitate and isotopic composition of organic compounds bound in diatoms frustules and sponge spicules in the environment.

SUPPORTING INFORMATION

Additional supporting information may be found in the online version of this article.

Acknowledgements

We thank Laura Truxal for assistance in the laboratory. Samples from TNO57-13 were provided by the repository at the Lamont-Doherty Earth Observatory. This work was supported by grants from the NSF OCE0525829 (AEI) and by the Gary C. Comer Science and Education Foundation.

REFERENCES

[1] T. Oshima. *J. Biol. Chem.* **1979**, *254*, 8720.
[2] K. Hamana, M. Niitsu, K. Samejima, S. Matsuzaki. *J. Biochem.* **1991**, *109*, 444.
[3] K. Hamana, S. Matsuzaki, M. Niitsu, K. Samejima. *Can. J. Bot.* **1994**, *72*, 1114.
[4] N. Kröger, R. Deutzmann, C. Bergsdorf, M. Sumper. *Proc. Natl. Acad. Sci.* **2000**, *97*, 14133.
[5] J. M. Knott. *FEBS Lett.* **2009**, *583*, 3519.
[6] N. Kröger, R. Deutzmann, M. Sumper. *Science* **1999**, *286*, 1129.
[7] M. Sumper. *Science* **2002**, *295*, 2430.
[8] M. Sumper, E. Brunner, G. Lehmann. *FEBS Lett.* **2005**, *579*, 3765.
[9] M. Sumper, E. Brunner. *Chem. Biochem.* **2008**, *9*, 1187.
[10] S. Matsunaga, R. Sakai, M. Jimbo, H. Kamiya. *Chem. BioChem.* **2007**, *8*, 1729.
[11] N. Kröger, N. Poulsen, in *Handbook of Biomineralization: Biological Aspects and Structure Formation*, (Eds: P. Behrens, E. Baeuerlein), Wiley-VCH, Weinheim, **2007**, pp. 43–58.
[12] A. E. Ingalls, R. F. Anderson, A. Pearson. *Mar. Chem.* **2004**, *92*, 91.
[13] M. C. Bridoux, A. I. Ingalls. *Geochim. Cosmochim. Acta* **2010**, *74*, 4044.
[14] L. G. Frigeri, T. R. Radabaugh, P. A. Haynes, M. Hildebrand. *Mol. Cell. Proteomics* **2006**, *5*, 182.
[15] M. Sumper, G. Lehmann. *Chem. Biochem.* **2006**, *7*, 1419.
[16] D. J. Belton, S. V. Patwardhan, V. V. Annenkov, E. N. Danilovtseva, C. C. Perry. *Proc. Natl. Acad. Sci.* **2008**, *105*, 5963.
[17] A. Bernecker, R. Wieneke, R. Riedel, M. Seibt, A. Geyer, C. Steinem. *J. Am. Chem. Soc.* **2010**, *132*, 1023.
[18] M. R. Häkkinen, T. A. Keinänen, J. Vepsäläinen, A. R. Khomutov, L. Alhonen, J. Jänne, S. Auriola. *J. Pharmaceut. Biomed. Anal.* **2007**, *45*, 625.
[19] V. V. Annenkov, S. N. Zelinskiy, E. N. Danilovtseva, C. C. Pery. *ARKIVOC* **2009**, *13*, 116.
[20] H. Menzel, S. Horstmann, P. Behrens, P. Barnreuther, I. Krueger, M. Jahns. *Chem. Commun.* **2003**, 2994.
[21] F. E. Kuhlmann, A. Apffel, S. M. Fischer, G. Goldberg, P. C. Goodley. *J. Am. Soc. Mass. Spectrom.* **1995**, *6*, 1221.
[22] W. Z. Shou, W. Naidong. *J. Chromatogr. B.* **2005**, *825*, 186.
[23] G. J. Feistner. *Biol. Mass. Spectrom.* **1994**, *23*, 784.
[24] L. Bigler, M. Hesse. *J. Am. Soc. Mass. Spectrom.* **1995**, *6*, 634.
[25] S. Chesnov, L. Bigler, M. Hesse. *Helvet. Chim. Acta* **2000**, *83*, 3295.
[26] M. Tzouros, N. Manov, S. Bienz, L. Gigler. *J. Am. Soc. Mass. Spectrom.* **2004**, *15*, 1636.

